

<https://www.revistas.espol.edu.ec/index.php/matematica/issue/archive>

Simulation of an optimal control problem of reservoir-people epidemiological model

Simulación de un problema de control óptimo del modelo epidemiológico reservorio-personas

Cristhian Alexander Núñez Ramos and Elisa Natalia Villacís Tulcán

Recepción: 05/05/2025 **Aceptación:** 11/07/2025 **Publicación:** 29/07/2025

Abstract This article studies an algorithm to solve an optimal control problem in a reservoir-people epidemiological model. The main objective of this work is to identify optimal vaccination and treatment strategies that can be implemented while minimizing the material and human costs associated with the epidemic. To achieve this, we use the Pontryagin's Maximum Principle, a mathematical result that provides the necessary conditions to find the characterization of the optimal control associated with ordinary differential equations.

Additionally, numerical simulations are performed to validate the proposed methodology. It provides a tool for decision-making and the efficient implementation of vaccination and treatment in epidemic scenarios, as well as facilitating the planning of responses to future public health crises.

Keywords epidemiological models · Hamiltonian · numerical simulations · optimal control · reservoir-people transmission model

2020 Mathematics Subject Classification 49K15 (primary) · 92C65 · 37M05

Resumen Este artículo estudia un algoritmo para resolver un problema de control óptimo en un modelo epidemiológico reservorio-personas. El principal objetivo de este trabajo es identificar estrategias óptimas de vacunación y tratamiento que puedan implementarse minimizando los costos materiales y humanos asociados con la epidemia. Para lograr esto, se utiliza el Principio del Máximo de Pontryagin, un resultado matemático que proporciona las condiciones necesarias para encontrar la caracterización del control óptimo asociado con ecuaciones diferenciales ordinarias. Además, se realizan simulaciones numéricas para validar la metodología propuesta. Proporciona una herramienta para la toma de decisiones y la implementación efi-

Cristhian Alexander Núñez Ramos (*)

Pontificia Universidad Católica de Chile, Facultad de Matemáticas, Santiago-Chile. e-mail: aanunez6@uc.cl, ORCID iD: <https://orcid.org/0009-0009-4659-6640>

Elisa Natalia Villacís Tulcán

Unidad Educativa Rafael Larrea Andrade, Comisión Técnico Pedagógica de Ciencias Naturales, Quito-Ecuador. e-mail: elisa.villacis@educacion.gob.ec, ORCID iD: <https://orcid.org/0009-0006-0595-7823>

ciente de la vacunación y el tratamiento en escenarios epidémicos, además de facilitar la planificación de respuestas ante futuras crisis de salud pública.

Palabras clave control óptimo · Hamiltoniano · modelo de transmisión reservorio-personas · modelos epidemiológicos · simulaciones numéricas

1 Introduction

In 1911, Ronald Ross developed a malaria model, contributing significantly to the field of disease transmission [20]. In 1927, Anderson Gray McKendrick and William Ogilvy Kermack developed a mathematical model to study the spread of the 1906 plague in India, which led to the formulation of the SIR (Susceptible-Infectious-Recovered) model [18]. Over time, advancements in mathematical epidemiology led to the development of the SEIR (Susceptible-Exposed-Infected-Recovered) model, which extends the SIR framework by incorporating an incubation period before individuals become infectious [6]. This approach allows for a more accurate representation of disease dynamics, making epidemiological models essential for understanding transmission patterns. The model choice depends on the disease's specific characteristics and the affected population. For example, COVID-19 and influenza are both respiratory illnesses, but different viruses cause them and have distinct characteristics. One key difference is their incubation periods, in COVID-19 (estimated 6.4 days) is longer than that of influenza type A (3.4 days) [17]. Understanding these characteristics, these models aim to analyze disease transmission dynamics and help create effective control strategies.

In late 2019, Wuhan-China, experienced an outbreak of Coronavirus Disease 2019 (COVID-19), caused by the novel coronavirus SARS-CoV-2. The outbreak rapidly expanded, affecting all regions of China and subsequently spreading worldwide. On March 11, 2020, the World Health Organization declared COVID-19 a pandemic [1]. This illness exhibits various clinical symptoms, including fever, dry cough, and fatigue, frequently accompanied by respiratory complications. Notably, SARS-CoV-2 is highly transmissible, and most of the general population remains susceptible to infection. The primary sources of the virus are wild animal hosts and then infected individuals, with transmission occurring primarily through respiratory droplets and direct contact [19].

In 2020, a Bats-Hosts-Reservoir-People (BHRP) transmission model of COVID-19 from a presumed source of infection (bats) to humans was proposed in [5]. The model uses 14 ordinary differential equations and 25 coefficients representing transition rates among 14 groups based on the SEIR model. The simplified Reservoir-People transmission model assumes that the virus was introduced to humans via a seafood market, excluding the bats-hosts route due to the unknown origin of the infection. This model can be adapted for other diseases with similar transmission patterns and can be used to formulate an optimal control problem to identify effective strategies for controlling the spread of disease.

The optimal control theory addresses controlling a system with variables that can be manipulated from the outside to achieve the best result. This theory can be applied in various fields like biology, economics, business, physics, and engineering, which involve using Ordinary Differential Equations (ODE). In particular, optimal control theory in the epidemiological field allows us to determine the most effective control to combat epidemics. This includes strategies such as isolation, treatment, and vaccination [1, 10], among others, to reduce infection rates and associated costs [13]. Characterizing the solution is one of the most challenging tasks in this field. In this sense, Pontryagin's Maximum Principle (PMP) emerges as a fundamental theory that provides optimality conditions, which can be used to characterize the solution [2, 11].

In this article, we present an algorithm to solve an optimal control problem based on the reservoir-people transmission model (RP) studied on [5], which describes the progression of an epidemic among five population groups. Disease transmission dynamics are analyzed in environments that act as sources of infection. We examine control strategies, such as vaccination and treatment, and apply optimal control theory and PMP to establish the conditions for optimal control. Finally, numerical simulations demonstrate the most effective application of vaccination and treatment strategies.

The article is structured as follows. Sect. 1.2 presents the problem statement for disease control using the model given in [5] and outlines the optimal control characterization using PMP [2]. In Sect. 1.3, numerical simulations are performed to identify suitable control strategies. The article ends with some final conclusions in Sect. 1.4.

2 Materials and Methods

This section presents the problem formulation, including an Ordinary Differential Equations (ODE) system and an objective function to minimize the application costs. Using Pontryagin's Maximum Principle, we then derive the characterization of the solution.

2.1 *Statement of the optimal control problem*

We introduce the reservoir-people epidemiological model, studied in [5], which simplifies the dynamics of a virus by excluding births and deaths unrelated to the disease or other external factors. The population is divided into five groups: susceptible individuals (S), exposed individuals (E), symptomatic infected individuals (I), asymptomatic infected individuals (A), and removed individuals (R), including both recovered and deceased individuals. The birth and death rates, represented by n and m , respectively, account for the inflow and outflow of individuals in the community.

The epidemiological model introduced in [5] considers the following parameters. The incubation and latent periods of human infection are represented as $1/w$ and $1/\bar{w}$, respectively. The model also incorporates the dynamics of the virus, which resides in a reservoir denoted by W that is the source of infection. Symptomatic and asymptomatic infected individuals can introduce the virus into W at rates μ and $\bar{\mu}$. The virus subsequently leaves the reservoir at a rate of ϵW , where $1/\epsilon$ represents the life period of the virus.

Furthermore, the durations of infection for the symptomatic (I) and asymptomatic (A) groups are characterized by $1/\gamma$ and $1/\bar{\gamma}$, respectively. The proportion of asymptomatic infections is denoted by δ , with the remaining fraction, $(1 - \delta)$, representing symptomatic infections. The susceptible group contracts the infection through contact with either W or the infected group I , with transmission rates denoted by b_W and b_P , respectively. The transmissibility of A is κ times that of I , where $0 \leq \kappa \leq 1$.

In this context, the optimal control problem introduces the functions u_1 and u_2 , which represent vaccination and treatment, respectively. These control functions aim to maximize the number of recovered individuals, minimize the number of infected and susceptible individuals, and reduce the costs associated with their implementation.

The parameters of the optimal control problem are detailed in Table 1.

Table 1 Parameters of the (RP) model

Notation	Description
A_1	The cost of vaccination
A_2	The cost of treatment
T	The infection timing
n	The birth and inflow rate of people
m	The death and outflow rate of people
b_P	The transmission rate from I to S
κ	The transmissibility of A with respect to that of I
b_W	The transmission rate from W to S
δ	The proportion of asymptomatic infections among the population
$(1 - \delta)$	The proportion of symptomatic infection rate of people
$1/w_P$	The incubation period experienced by individuals
$1/\gamma$	The duration of the infectious period for symptomatic individuals.
$1/\bar{w}$	The latent period of people
$1/\bar{\gamma}$	The duration of the infectious period for asymptomatic people
$1/e$	The virus lifespan in W
c	The relative shedding coefficient of A compared to I

Figure 1 illustrates disease dynamics, with the interaction between the reservoir and the human population. It also includes control strategies (vaccination and treatment). W represents the reservoir where the virus resides and multiplies. The five compartments of the population are susceptible (S), exposed (E), symptomatic (I), asymptomatic (A), and removed (R) people. Arrows illustrate the flow of individuals between compartments. The diagram includes parameters that are essential for mod-

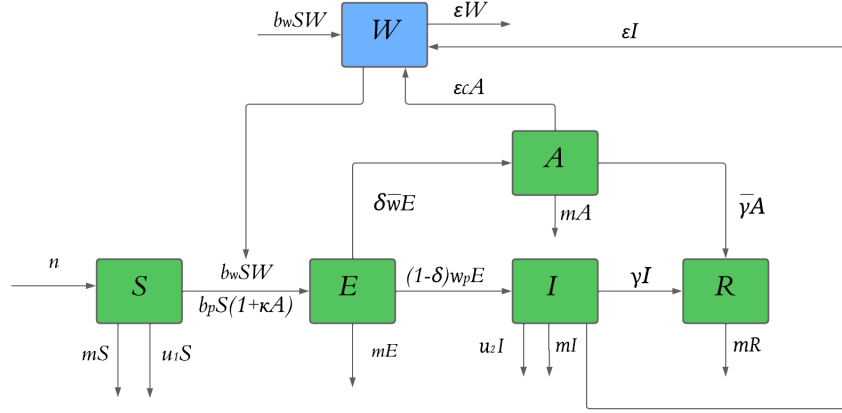


Fig. 1 Framework of the Optimal Control Problem

elting the dynamics of disease transmission and assessing the impact of the controls u_1 and u_2 on controlling the spread of infections originating from the reservoir.

The optimal control problem (**OPC**) is the following

$$\min_{(u_1, u_2) \in \mathbb{U}} J(u_1(t), u_2(t)) = \begin{cases} S(T) + I(T) - R(T) \\ + \int_0^T \left(\frac{\lambda_1}{2} u_1^2(t) + \frac{\lambda_2}{2} u_2^2(t) + S(t) + I(t) - R(t) \right) dt \end{cases}$$

subject to:

$$(\mathbf{RP}) \begin{cases} \dot{S} = n - mS - b_p S(I + \kappa A) - b_W SW - u_1 S, \\ \dot{E} = b_p S(I + \kappa A) + b_W SW - (1 - \delta) w_p E \\ \quad - \delta \bar{w} E - mE, \\ \dot{I} = (1 - \delta) w_p E - (\gamma + m) I - u_2 I, \\ \dot{A} = \delta \bar{w} E - (\bar{\gamma} + m) A, \\ \dot{R} = \gamma I + \bar{\gamma} A - mR, \\ \dot{W} = \epsilon(I + cA - W). \end{cases}$$

This includes an objective function J , which will be minimized subject to the reservoir-people model. The objective function considers both the time interval and the final state, emphasizing reducing the susceptible and infected groups while increasing the number of recovered individuals at the final time.

The functions $u_1(t)$ and $u_2(t)$ denote vaccination and treatment strategies, respectively. The set of admissible controls is

$$\mathbb{U} = \{(u_1, u_2) \in (L^\infty(0, T))^2 : a_1 \leq u_1(t) \leq b_1, a_2 \leq u_2(t) \leq b_2\}, \quad (1)$$

where $0 \leq a_1 < b_1 \leq 1$ and $0 \leq a_2 < b_2 \leq 1$. The two constants λ_1 and λ_2 represent the costs associated with the use of controls $u_1(t)$ and $u_2(t)$, respectively. This means that as the value of either constant increases, the cost of applying the corresponding control also rises.

Besides, the objective function is a quadratic function, which implies that it is a convex function. Consequently, the existence of the solution is derived from the Filippov-Cesari theorem [7, 15, 11].

2.2 Characterization of the solution

In this subsection, we derive the first-order optimality conditions by constructing the Hamiltonian \mathcal{H} and applying PMP. The PMP provides the necessary conditions for solving optimal control problems by transforming the problem into a system of equations that include adjoint variables. These adjoint variables characterize the optimal control problem, and the control is obtained by minimizing the Hamiltonian with respect to these variables [2, 11].

We simplify the notation in the following way

$$\begin{aligned}\mathbf{x}(t) &= [S(t), E(t), I(t), A(t), R(t), W(t)]^T, \\ \mathbf{u}(t) &= [u_1(t), u_2(t)]^T, \\ \mathbf{p}(t) &= [p_1(t), p_2(t), p_3(t), p_4(t), p_5(t), p_6(t)]^T,\end{aligned}$$

and the Hamiltonian is expressed as:

$$\begin{aligned}\mathcal{H} &= \frac{\lambda_1}{2}u_1^2 + \frac{\lambda_2}{2}u_2^2 + S + I - R + p_1(n - mS - b_p S(I + \kappa A) - b_W SW - u_1 S) \\ &\quad + p_2(b_p S(I + \kappa A) + b_W SW - (1 - \delta)w_p E - \delta \bar{w} E - mE) \\ &\quad + p_3((1 - \delta)w_p E - (\gamma + m)I - u_2 I) \\ &\quad + p_4(\delta \bar{w} E - (\bar{\gamma} + m)A) \\ &\quad + p_5(\gamma I + \bar{\gamma} A - mR) \\ &\quad + p_6(\epsilon(I + cA - W))\end{aligned}\tag{2}$$

which includes the control and the state variables, $\mathbf{u}^* = [u_1^*, u_2^*]^T$ and $\mathbf{x}^*(t) = [S^*(t), E^*(t), I^*(t), A^*(t), R^*(t), W^*(t)]^T$, respectively. Besides, the Hamiltonian given by Equation 2 introduces an adjoint state $\mathbf{p}(t)$, which serves to characterize the optimal control. The PMP ensures that the solution satisfies

$$\frac{\partial \mathcal{H}}{\partial \mathbf{u}}(t) = 0, \quad \dot{\mathbf{x}}(t) = \frac{\partial \mathcal{H}}{\partial \mathbf{p}}(t), \quad \dot{\mathbf{p}}(t) = -\frac{\partial \mathcal{H}}{\partial \mathbf{x}}(t).$$

The optimality conditions for the problem are:

$$\left[\frac{\partial \mathcal{H}}{\partial u_1}(t) \right]_{\mathbf{u}(t)=\mathbf{u}^*} = 0, \quad \left[\frac{\partial \mathcal{H}}{\partial u_2}(t) \right]_{\mathbf{u}(t)=\mathbf{u}^*} = 0,$$

and then replacing the above conditions, we obtain:

$$\lambda_1 u_1^*(t) - S(t)p_1(t) = 0, \quad \lambda_2 u_2^*(t) - I(t)p_3(t) = 0. \quad (3)$$

Besides, by considering $\mathbf{u}^* \in \mathbb{U}$ (Equation 1), then the writing of Equations 3 can be simplified respectively, as follows:

$$u_1^*(t) = \min \left\{ b_1; \max \left\{ a_1; \frac{S(t)p_1(t)}{\lambda_1} \right\} \right\}, \quad u_2^*(t) = \min \left\{ b_2; \max \left\{ a_2; \frac{I(t)p_3(t)}{\lambda_2} \right\} \right\}.$$

The state equations are given by **(RP)**, and the adjoint equations are written like:

$$\begin{aligned} \dot{p}_1(t) &= -\frac{\partial \mathcal{H}}{\partial S}(t), & \dot{p}_2(t) &= -\frac{\partial \mathcal{H}}{\partial E}(t), & \dot{p}_3(t) &= -\frac{\partial \mathcal{H}}{\partial I}(t), \\ \dot{p}_4(t) &= -\frac{\partial \mathcal{H}}{\partial A}(t), & \dot{p}_5(t) &= -\frac{\partial \mathcal{H}}{\partial R}(t), & \dot{p}_6(t) &= -\frac{\partial \mathcal{H}}{\partial W}(t), \end{aligned}$$

which are equivalent to

$$\begin{aligned} \dot{p}_1(t) &= -1 + mp_1 + b_p p_1(I + \kappa A) + b_W p_1 W + u_1 p_1 - b_p p_2(I + \kappa A) - b_W p_2 W, \\ \dot{p}_2(t) &= p_2(1 - \delta)w_p + \delta p_2 \bar{w} + mp_2 + p_3(\delta - 1)w_p - \delta \bar{w} p_4, \\ \dot{p}_3(t) &= -1 + b_p S(p_1 - p_2) + (\gamma + m + u_2)p_3 - \gamma p_5 - \epsilon p_6, \\ \dot{p}_4(t) &= b_p \kappa S(p_1 - p_2) + p_4(\bar{\gamma} + m) - \bar{\gamma} p_5 - \epsilon c p_6, \\ \dot{p}_5(t) &= 1 + mp_5, \\ \dot{p}_6(t) &= b_W S(p_1 - p_2) + \epsilon p_6. \end{aligned}$$

The adjoint equations are completed with the following transversality conditions at final time:

$$p_1(T) = 1, \quad p_2(T) = 0, \quad p_3(T) = 1, \quad p_4(T) = 0, \quad p_5(T) = -1, \quad p_6(T) = 1.$$

3 Results and Discussion

This section presents numerical simulations of the solution of the optimal control problem using the approach presented in the above section. The code was generated in MATLAB and is available in [16]

3.1 Numerical simulations

The parameters for the numerical simulations correspond to the transmission of SARS-CoV-2 in Wuhan City during 2020. Next, we estimate the parameters using the following facts and assumptions [4, 5, 12].

- The mean incubation period is 5.2 days. We assume that the incubation period and the latent period are the same. Thus, $w_p = \bar{w} = 0.1923$, see [4].
- There is an average delay of 5 days between symptom onset and case detection or hospitalization. The estimated mean duration from illness onset to the first medical visit is 5.8 days. In this study, the infectious period is assumed to be 5.8 days, leading to $\gamma = 0.1724$, [4].
- Due to the lack of data on the proportion of asymptomatic infections, we set a baseline value of 0.5 for the simulation, that is, $\delta = 0.5$. It serves as a starting point for the model, but it is important to note that this is a hypothetical assumption made in the absence of real data on asymptomatic infections.
- In the absence of evidence on the transmissibility of asymptomatic infections, we assume it to be 0.5 times that of symptomatic infections ($\kappa = 0.5$), similar to the value observed for influenza [12]. Additionally, we assume that the relative shedding rate of A compared to I is 0.5, leading to $c = 0.5$.
- Based on the number of body temperature screenings of passengers, mobility studies, and population data collected in Wuhan in January 2020, the rate of people traveling from Wuhan is set at 0.00018. Consequently, the rate of people entering and exiting Wuhan is taken as 0.00018 per day ($n = m = 0.00018$), see [5].
- The parameters b_p and b_W were estimated to align the model's outputs as closely as possible with real-world observational data, c.f. [5].
- At the start of the simulation, we assume the virus prevalence in the market to be 1 in 100,000. This assumption provides an initial condition that allows the model to simulate the disease dynamics starting with a low level of infection.
- Since SARS-CoV-2 is an RNA virus, we assume it degrades quickly in the environment but can persist for a longer period (up to 10 days) in unknown hosts in a crowded place. We set $\epsilon = 0.1$, which represents the rate at which viral viability decays in the environment or within hosts.

Furthermore, it is assumed that only 30% of the population is subjected to vaccination and treatment processes, meaning that $a_1 = 0$, $a_2 = 0$, $b_1 = 0.3$, and $b_2 = 0.3$.

The complete selection of parameters for the numerical simulations is detailed in Table 2.

Table 2 Parameters estimation

Parameter	Numerical value	Parameter	Numerical value
λ_1	1.0000	λ_2	1.0000
T	10.000	n	0.0018
m	0.0018	b_P	0.5000
κ	0.5000	b_W	0.8000
δ	0.5000	w_P	0.1923
γ	0.1724	\tilde{w}	0.1923
$\tilde{\gamma}$	0.1724	ϵ	0.1000
c	0.5000		

Now, we introduce an algorithm to solve (**OCP**), which can be extended to many similar problems. Specifically, we combine the characterization obtained through PMP with Algorithm 1, based in [9]. The main complication arises because the state equation is defined at the initial time, while the adjoint equation is defined at the final time. This results in a non-trivial computational challenge for solving the optimal control problem.

Algorithm 1: Algorithm for solving (OCP)

Input: Initial conditions and parameters
Output: Controls
Result: Optimal controls

Initialization;
for $i = -\mathcal{M}, \dots, 0$ **do**
 $S_i = S_0; E_i = E_0; I_i = I_0; A_i = A_0; R_i = R_0; W_i = W_0; u_1^i = 0; u_2^i = 0;$
end
for $i = \mathcal{M}, \dots, 2\mathcal{M}$ **do**
 $p_1^i = 1; p_2^i = 0; p_3^i = 1; p_4^i = 0; p_5^i = -1; p_6^i = 0;$
end
Main iteration;
for $i = 0, \dots, \mathcal{M} - 1$ **do**
 $S_{i+1} = S_i + h[n - mS_i - b_p S_i(I_i + \kappa A_i) - b_W S_i W_i - u_1^i S_i];$
 $E_{i+1} = E_i + h[b_p S_i(I_i + \kappa A_i) + b_W S_i W_i - (1 - \delta)w_p E_i - \delta \bar{w} E_i - m E_i];$
 $I_{i+1} = I_i + h[(1 - \delta)w_p E_i - (\gamma + m)I_i - u_2^i I_i];$
 $A_{i+1} = A_i + h[\delta \bar{w} E_i - (\bar{\gamma} + m)A_i]; R_{i+1} = R_i + h(\gamma I_i + \bar{\gamma} A_i - m R_i);$
 $W_{i+1} = W_i + h[\epsilon(I_i + c A_i - W_i)];$
 $p_1^{M-i-1} = p_1^{M-i} - h[-1 + m p_1^{M-i} + b_p p_1^{M-i}(I_{i+1} + \kappa A_{i+1}) +$
 $b_W p_1^{M-i} W_{i+1} + u_1^i p_1^{M-i} - b_p p_2^{M-i}(I_{i+1} + \kappa A_{i+1}) - b_W p_2^{M-i} W_{i+1}];$
 $p_2^{M-i-1} = p_2^{M-i} - h[p_2^{M-i}(1 - \delta)w_p + \delta p_2^{M-i} \bar{w} + m p_2^{M-i} + p_3^{M-i}(\delta -$
 $1)w_p - \delta \bar{w} p_4^{M-i}]; p_3^{M-i-1} = p_3^{M-i} - h[-1 + b_p S_{i+1}(p_1^{M-i} - p_2^{M-i}) +$
 $(\gamma + m + u_2^i)p_3^{M-i} - \gamma p_5^{M-i} - \epsilon p_6^{M-i}]; p_4^{M-i-1} =$
 $p_4^{M-i} - h[b_p \kappa S_{i+1}(p_1^{M-i} - p_2^{M-i}) + p_4^{M-i}(\bar{\gamma} + m) - \bar{\gamma} p_5^{M-i} - \epsilon c p_6^{M-i}];$
 $p_5^{M-i-1} = p_5^{M-i} - h[1 + m p_5^{M-i}];$
 $p_6^{M-i-1} = p_6^{M-i} - h[b_W S_{i+1}(p_1^{M-i} - p_2^{M-i}) + \epsilon p_6^{M-i}];$
 $u_1^{i+1} = \min\{b_1; \max\{a_1; \frac{S_{i+1} p_1^{M-i}}{\lambda_1}\}\};$
 $u_2^{i+1} = \min\{b_2; \max\{a_2; \frac{I_{i+1} p_3^{M-i}}{\lambda_2}\}\};$
end
Final results;
for $i = 1, \dots, \mathcal{M}$ **do**
 $S^*(t_i) = S_i; E^*(t_i) = E_i; I^*(t_i) = I_i; A^*(t_i) = A_i; R^*(t_i) = R_i;$
 $W^*(t_i) = W_i; u_1^*(t_i) = u_1^i; u_2^*(t_i) = u_2^i;$
end

Algorithm 1 is a numerical variant of the forward Euler method, incorporating a step size and integrating temporal iterations for both state and adjoint equations; review [9, 3, 14] for further information.

3.2 Graphical summaries and Comments

Figure 2 illustrates the dynamics of the susceptible population under different scenarios: no control (red line), treatment only (blue line), vaccination only (brown line), and both controls (green line). In the no-control scenario, both $u_1 = 0$ and $u_2 = 0$. The blue line represents the population with treatment but no vaccination ($u_1 = 0$ and $u_2 \neq 0$). The brown line shows the dynamics when only vaccination is applied ($u_1 \neq 0$ and $u_2 = 0$). The green curve corresponds to the case where both vaccination and treatment are used ($u_1 \neq 0$ and $u_2 \neq 0$). This last scenario highlights that, without vaccination, many people remain virus carriers. However, with treatment alone, susceptibility is higher than in the no-control scenario because individuals who recover from the infection may become susceptible again.

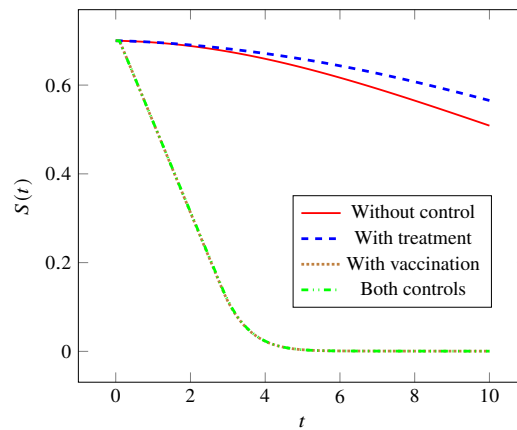


Fig. 2 Evolution of susceptible population under different control strategies

Figure 3 shows the dynamics of the exposed population under different control combinations, similar to the previous case. Using only treatment control reduces the number of exposed individuals, but vaccination plays a key role in further decreasing the size of the exposed group. As in the susceptible population case, many individuals remain exposed without vaccination. No significant differences are observed in the exposed population when vaccination control is added to the treatment scenario. In conclusion, vaccination notably reduces the number of exposed individuals.

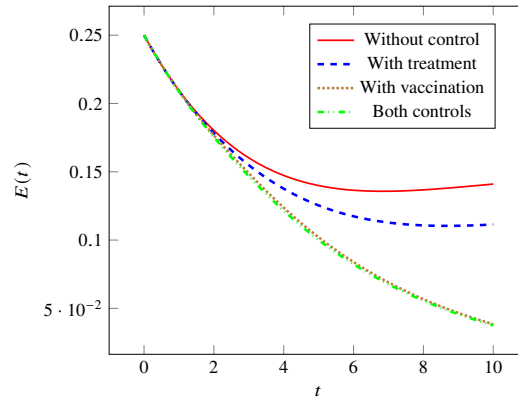


Fig. 3 Evolution of exposed population under different control strategies

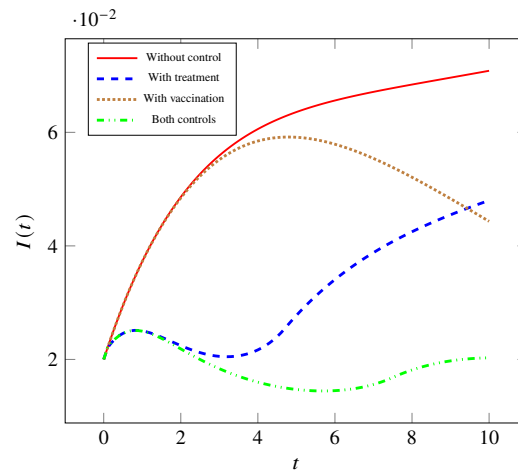


Fig. 4 Evolution of infected population under different control strategies

Figure 4 shows the behavior of the infected group under different control strategies, highlighting the effectiveness of vaccination in the susceptible population and treatment in the infected group. The intersection point between the blue and brown lines illustrates the interaction between both control strategies, which can be explained by the dynamics of the model (RP). This helps us assess each control's performance based on its application's timing. Vaccination is crucial in reducing the number of infected individuals, even when treatment is applied. For instance, we observe an increase in the infected group in the blue line, representing the scenario where only treatment is applied. The green line assures the importance of using both controls to rapidly and effectively reduce the infected population. Figure 5 shows

that the number of asymptomatic individuals increases in the absence of vaccination, which is expected since vaccination acts before infection. This difference becomes more noticeable later in time, specifically for $t > 3$. Both controls are effective, but vaccination has a more significant impact than treatment on asymptomatic individuals.

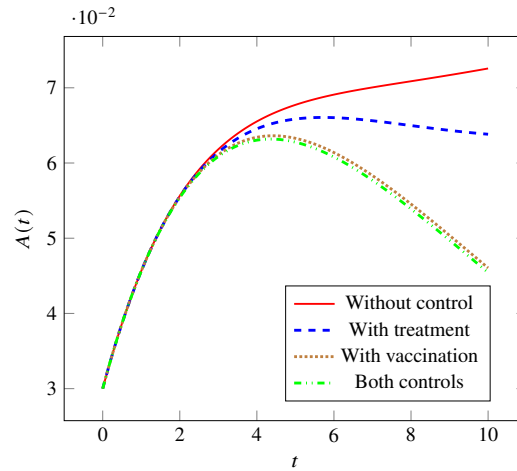


Fig. 5 Evolution of asymptomatic population under different control strategies

The effectiveness of treatment and preventive vaccination is shown in the removed case (recovered and deceased) in Figure 6. The interpretation of this figure requires careful consideration, as a higher number of removed individuals does not necessarily indicate that more people are being saved; in fact, it could suggest the opposite. Vaccination directly influences the recovered group by preventing a rapid increase in infections. Notably, the number of removed individuals is the highest in the red scenario (no control). In this case, we interpret as those who could not recover from the disease (deceased) and were removed from the system.

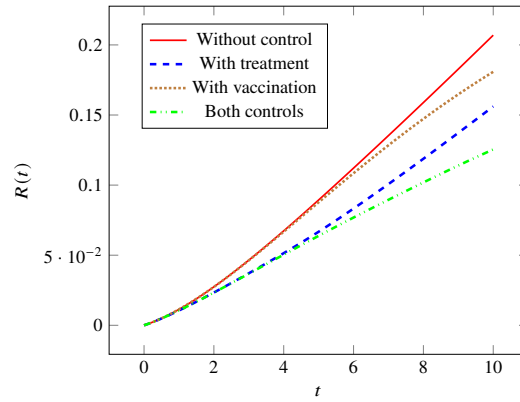


Fig. 6 Evolution of removed population under different control strategies

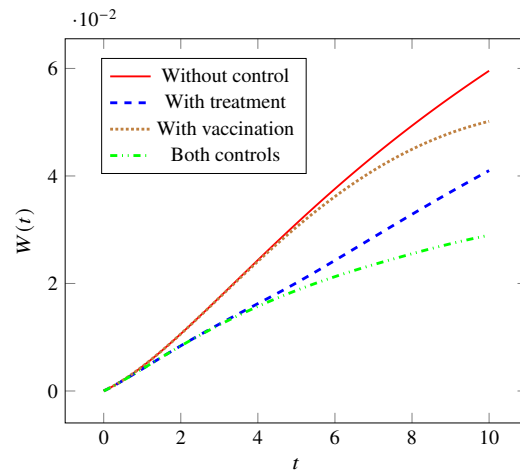


Fig. 7 Evolution of virus under different control strategies

Figure 7 illustrates the virus dynamics in the reservoir. A reduction in virus density is achieved through vaccination and treatment. In this analysis period, treatment has a greater effect than vaccination, as infected individuals transmit the virus directly into the reservoir. However, analyzing the trends of the curves, vaccination will play a more prominent role over a longer period.

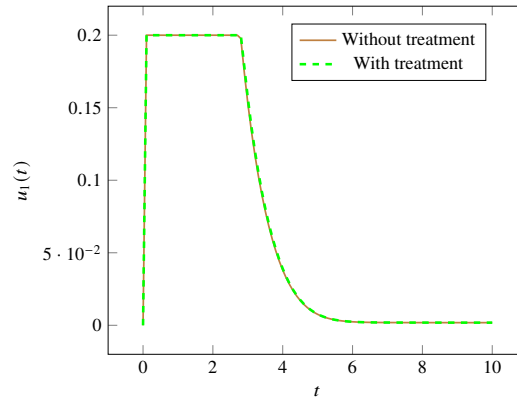


Fig. 8 Optimal vaccination dynamics with and without treatment during an epidemic

Regarding control functions, Figure 8 illustrates the vaccination control when applied (either alone or in combination with treatment). When vaccination is activated, it operates at full capacity — 30%, as predetermined — which aligns with similar cases in [14]. The control is most effective at the beginning of the epidemic and gradually decreases as the number of susceptible individuals declines.

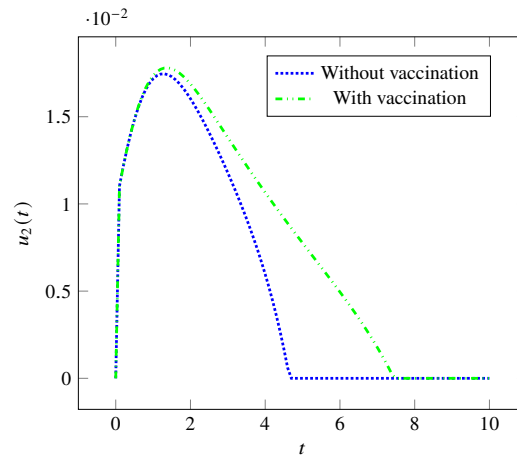


Fig. 9 Optimal treatment dynamics with and without vaccination during an epidemic

However, treatment control behaves differently when combined with vaccination. As shown in Figure 9, treatment is no longer necessary after a certain point. In the blue scenario, where only treatment is applied, it is effective before $t = 5$. However, when combined with vaccination, its effectiveness extends beyond $t = 7$. This highlights the difference between using both controls simultaneously versus individually.

4 Conclusions

This study examined an optimal control problem for a disease transmission model between reservoirs and populations, aiming to minimize infection rates while optimizing the use of vaccination and treatment strategies. By formulating a mathematical framework and applying Pontryagin's maximum principle, we characterized the optimal control strategies and validated their effectiveness through numerical simulations.

The results highlight vaccination's crucial role in reducing the number of susceptible, exposed, and infected individuals. Preventive measures significantly decrease the spread of the disease, whereas treatment alone, while beneficial, may not be sufficient to control the epidemic effectively. Combining both controls proves to be the most effective strategy, leading to a faster and more reduction in infection.

Another key finding is that the interpretation of removed cases requires careful consideration. A higher number of removed individuals does not necessarily imply better health outcomes, as it may include individuals who did not survive the disease. This reinforces the importance of preventive measures in reducing mortality.

The study also emphasizes the dynamic nature of control strategies. Vaccination efforts are most impactful at the beginning of an outbreak, gradually decreasing as the number of susceptible individuals declines. Meanwhile, treatment strategies show varying levels of effectiveness depending on their timing and whether they are combined with preventive measures. The interplay between these interventions highlights the importance of adaptive strategies rather than static ones.

From a methodological perspective, implementing numerical algorithms to solve the optimal control problem allowed for an efficient identification of cost-effective strategies. The approach presented in this study provides a framework that can be adapted to real-world scenarios, offering insights into the optimal allocation of healthcare resources during epidemics.

In future work, a sensitivity analysis can be conducted concerning the key parameters of the model, particularly the person-to-person transmission rate (b_p) and the effectiveness of treatment (u_2). Evaluating the influence of these parameters on the system's dynamics will provide a better understanding of the epidemic's stability under different control strategies. This study would help identify critical thresholds where vaccination and treatment are most effective, offering valuable insights for decision-making in real epidemiological contexts. Besides, future research could focus on refining the model by incorporating real-world data, improving parameter estimation, and considering additional constraints to better reflect practical limitations in vaccination and treatment deployment. Additionally, exploring the impact of control strategies under different epidemiological conditions could further enhance the applicability of the findings to various public health contexts, see e.g [8].

References

1. Aslan, I.H., Demir, M., Wise, M.M. and Lenhart, S.: *Modeling COVID-19: forecasting and analyzing the dynamics of the outbreaks in Hubei and Turkey*, *Mathematical Methods in the Applied Sciences* **45**, 6481–6494 (2022)
2. Badescu, V.: *Optimal Control in Thermal Engineering*, *Studies in Systems, Decision and Control*, Springer, 89–109 (2017)
3. Barro, M., Aboudramane, G. and Ouedraogo, D.: *Optimal control of a SIR epidemic model with general incidence function and time delays*, *Cubo* **20**, 53–66 (2018)
4. Chen, T., Yang, J., Zhang, R., Li, X., Ma, J. and Yang, G.: *The transmissibility estimation of influenza with early stage data of small-scale outbreaks in Changsha, China, 2005–2013*, *Epidemiology and Infection* **145**, 1–10 (2016)
5. Chen, T. M., Guo, J., Li, M., Wu, L., Zhang, Z. and Wang, Y.: *A mathematical model for simulating the phase-based transmissibility of a novel coronavirus*, *Infectious Diseases of Poverty* **9** (2020)
6. Dansana, D., Gupta, V., Singh, A., Sharma, R., Soni, N. and Jain, R.: *Using Susceptible-Exposed-Infectious-Recovered Model to Forecast Coronavirus Outbreak*, *Computers, Materials and Continua* **67**, 1595–1612 (2021)
7. Gerdt, M.: *Optimal Control of Ordinary Differential Equations and Differential-Algebraic Equations*, Habilitation, University of Bayreuth (2006)
8. Howerton, E., Rojas, D., Meeker, J. and Wilson, H.: *The effect of governance structures on optimal control of two-patch epidemic models*, *Journal of Mathematical Biology* (2023), in press
9. Laarabi, H., Karama, A., Benabdallah, H., and Abdelkader, S.: *Optimal Control of a Delayed SIRS Epidemic Model with Vaccination and Treatment*, *Acta Biotheoretica* **63**, 87–97 (2015)
10. Lacy, A., Bell, G., Ibarra, G., and Watson, L.: *Modeling impact of vaccination on COVID-19 dynamics in St. Louis*, *Journal of Biological Dynamics* **17**, 25 (2023)
11. Lenhart, S. and Workman, J.T.: *Optimal control applied to biological models*, Chapman and Hall/CRC (2007)
12. Longini, I.M., Halloran, M.E., Nizam, A., Yang, Y. and Gonçalves, M.: *Containing Pandemic Influenza at the Source*, *Science* **309**, 1083–1087 (2005)
13. Miller Neilan, R. and Lenhart, S.: *An Introduction to Optimal Control with an Application in Disease Modeling*, DIMACS Series in Discrete Mathematics **75**, (2010)
14. Maurer, H., Altrogge, I. and Goris, N.: *Optimization methods for solving bang-bang control problems with state constraints and the verification of sufficient conditions*, *Proceedings of the 44th IEEE Conference on Decision and Control*, 923–928 (2006)
15. Nababan, S.: *A Filippov-type lemma for functions involving delays and its application to time-delayed optimal control problems*, *Journal of Optimization Theory and Applications* **27**, 357–376 (1979)
16. Núñez, C.: *MATLAB code for computing the optimal control of the epidemiological reservoir-people model* (2025)
17. Pormohammad, A., Ghasemi, S. and Mehr, S.: *Comparison of influenza type A and B with COVID-19: A global systematic review and meta-analysis on clinical, laboratory and radiographic findings*, *Reviews in Medical Virology* **31**, e2179 (2021)
18. Rahimi, I., Chen, F., Gandomi, A. and Saeed, S.: *A review on COVID-19 forecasting models*, *Neural Computing and Applications* **35**, (2021)
19. Shi, Y., Wang, X., Jiang, H. and Luo, J.: *An overview of COVID-19*, *Journal of Zhejiang University Science B* **21**, 343–360 (2020)
20. Velasco-Hernandez, J.: *Modelos matematicos en epidemiologia: enfoques y alcances*, *Miscelanea Matematica* **44**, 11–27 (2007)